Oblique water entry of a wedge with vortex shedding

G.D. Xu[a]; G.X. Wu[a,b*]

[a]College of shipbuilding engineering, Harbin Engineering University, Harbin China (xuguodong@hrbeu.edu.cn)

[b]Permanent address: Department of Mechanical Engineering, University College London, Torrington Place, London WC1E 7JE, UK (author for correspondence: g.wu@ucl.ac.uk)

highlights:

- oblique water entry of a wedge with vortex wake is simulated
- the Kutta condition is imposed at the wedge apex and the local pressure jump is removed

1. Introduction

Wedge water entry is one of the most typical fluid/structure impact problems. For water entry of a symmetric wedge with only vertical motion, Howison et al. (1991), Mei et al. (1999), Korobkin & Iafrati (2005) presented the analytical solutions based on the Wagner theory; Dobrovol'skaya (1969) considered the fully nonlinear similarity solution; Zhao & Faltinsen (1993), Lu et al (1999), Wu et al (2004), Battistin & Iafrati (2003) simulated the nonlinear impact through the boundary element method (BEM). For water entry of an asymmetric wedge or oblique water entry, typical work include those by Iafrati & Semenov (2006) and Xu et al (2008, 2010). In their results pressure jump was observed at the wedge apex. As there is transverse flow passing the sharp corner, such discontinuity or singularity in the potential flow was not unexpected. In real flow there would be strong vortex shedding at a sharp corner. To simulate water entry of a wedge with transverse flow at its tip, flow separation due to vortex shedding needs to be treated properly. Riccardi & Iafrati (2004) investigated the vortex shedding of the water entry of an asymmetric wedge through conformal mapping, although the effect of the free surface elevation was ignored. Point vortex and Kutta condition were introduced to remove the velocity singularity at the apex.

The general problem of vortex shedding at a sharp corner of a marine structure has been receiving extensive attentions. Downie et al (1988) studied the vortex shedding of a rectangular barge in waves. Kristiansen & Faltinsen (2010) simulated the vortex shedding of a rectangular box in waves through BEM. The damping effects due to the shed vortices were accounted for properly. However, it seems that there is far less work in the context of water entry of a wedge, which is the focus of the present study. A Kutta condition for numerical simulation is imposed at the sharp edge. The pressure jump at the wedge apex is removed. Results for the free surface profile and pressure distribution are provided.

2. Mathematic equations

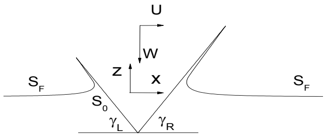

(a)

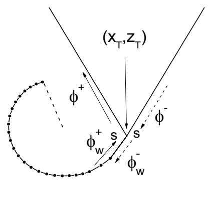

(b)

Fig.1 illustration of (a) the wedge water entry with vortex shedding and (b) the local wake surface

The velocity potential theory is adopted to describe the flow field since the viscosity and compressibility effects are less important during high speed water entry over a short period of time. As shown in Fig.(1a), the origin of the space-fixed Cartesian coordinate system $x-o-z$ is located on the initially calm water surface with z pointing upwards. The introduced velocity potential ϕ satisfies Laplace equation in the fluid domain

$$\nabla^2\phi = \frac{\partial^2\phi}{\partial x^2} + \frac{\partial^2\phi}{\partial z^2} = 0 \tag{1}$$

On the body surface S_0, the boundary condition can be written as

$$\frac{\partial\phi}{\partial n} = \vec{U}\cdot\vec{n} \tag{2}$$

where $\vec{U} = (U, W)$ is the translational constant velocity of the body and $\vec{n} = (n_x, n_z)$ is the unit normal vector pointing out of the fluid domain. In the Lagrangian framework, the free surface boundary conditions can be written as

$$\frac{d\phi}{dt} = \frac{1}{2}\nabla\phi\nabla\phi \tag{3}$$

$$\frac{dx}{dt} = \frac{\partial\phi}{\partial x}, \quad \frac{dz}{dt} = \frac{\partial\phi}{\partial z} \tag{4}$$

When there is transverse flow at the wedge apex, vortex wake will be shed into the fluid. On the wake surface S_w, the dipole strength can be written as

$$\mu = \phi_w^+ - \phi_w^- \tag{5}$$

while the normal velocity across S_w is continuous, or

$$\frac{\partial\phi_{w+}}{\partial n} = -\frac{\partial\phi_{w-}}{\partial n} \tag{6}$$

In Eq.(5) ϕ_w^+ and ϕ_w^- are the velocity potentials on the two sides of the wake surface, as shown in Fig.(1b). At the apex of the wedge, we impose the Kutta condition in the following form (Xu & Wu 2013)

$$\left.\frac{\partial\phi^+}{\partial l}\right|_{\vec{x}_{apex}} - \left.\frac{\partial\phi^-}{\partial l}\right|_{\vec{x}_{apex}} = \left.\frac{\partial\mu}{\partial l}\right|_{\vec{x}_{apex}} \tag{7}$$

where the tangential vector in $\left.\frac{\partial\mu}{\partial l}\right|_{\vec{x}_{apex}}$ has the same direction as $\left.\frac{\partial\phi^+}{\partial l}\right|_{\vec{x}_{apex}}$, as shown in Fig.(1b). The continuity of the pressure p across the wave surface gives

$$\frac{d\mu}{dt} = 0 \tag{8}$$

We notice that the wedge water entry problem usually starts from a contact point. An ideal approach is to use the stretched coordinate system (Wu et al 2004). It has the advantage that both the computational domain and the element size remain similar size in the stretched system as body continues to enter water in the physical domain. We define

$$s = Wt, \quad h = Ut \tag{9}$$

In the stretched coordinate system $\alpha - o - \beta$, we write

$$\phi(x, y, t) = s\varphi(\alpha, \beta, t), \quad x = s\alpha, \; y = s\beta \tag{10}$$

Laplace equation in the stretched system retains the same form, while the body surface boundary condition becomes

$$\frac{\partial\varphi}{\partial n} = Un_\alpha - Wn_\beta \tag{11}$$

and the free surface boundary conditions can be written as

$$\frac{d(s\alpha)}{dt} = \varphi_\alpha, \quad \frac{d(s\beta)}{dt} = \varphi_\beta \tag{12}$$

$$\frac{d(s\varphi)}{dt} = \frac{1}{2}(\varphi_\alpha^2 + \varphi_\beta^2) \tag{13}$$

To solve the above equations, following the numerical procedure of Xu & Wu (2013), we have the boundary integral equation at $m+1$ time step

$$\begin{aligned}\Lambda(p)\varphi(p) &= \int_{S_0+S_F} [\frac{\partial G(p,q)}{\partial n_q}\varphi(q) - G(p,q)\frac{\partial \varphi(q)}{\partial n_q}]dS \\ &+ \int_{S_{w1}} \frac{\partial G(p,q)}{\partial n_w}\mu'(q)\, dS + \mu'(\bar{\alpha}'_T)H(p,\bar{\alpha}'_T) + \sum_{j=1}^{m} k_j H(p,q)dS\end{aligned} \tag{14}$$

where $H(p,q) = \arctan\frac{\alpha-\xi}{\beta-\eta}$, S_{w1} is the dipole element attached to the sharp edge, κ_j is the point vortex formed from vortex dipole element in the $(j-1)th$ time step.

3. Results and discussions

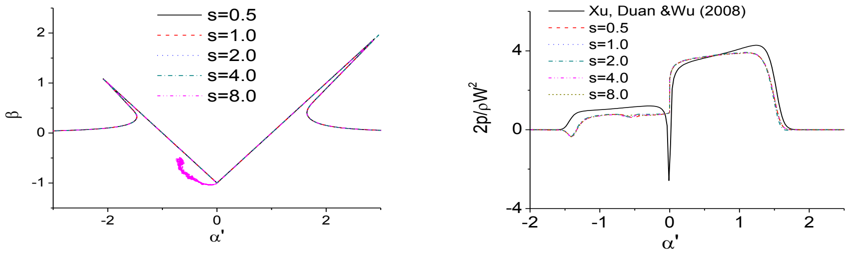

(a) (b)

Fig.2 oblique water entry of a wedge, (a) free surface profile and (b) the pressure distribution, $\alpha' = \alpha - \varepsilon$

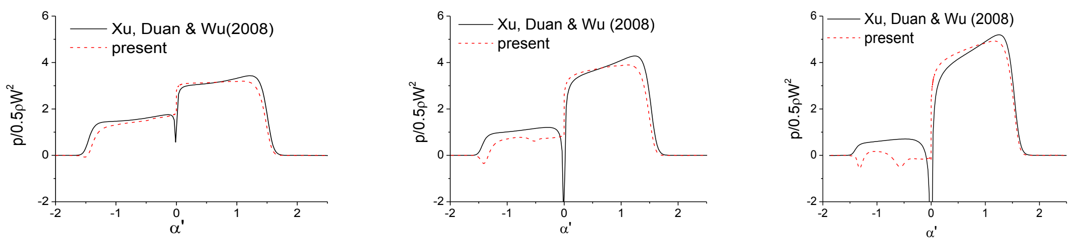

(a) (b) (c)

Fig.3 oblique wedge water entry with $\gamma_L = \gamma_R = \pi/4$, $s = 1.0$, (a) $\varepsilon = 0.3$(b) $\varepsilon = 0.5$ (c) $\varepsilon = 0.7$

The work is still on-going and only some preliminary results from the simulation are presented here. Oblique water entry of a symmetric wedge at constant velocity with left and right deadrise angles $\gamma_L = \gamma_R = \pi/4$, $\varepsilon = U/W = 0.5$ is considered. The initial free surface profile and the velocity potential are prescribed at $s = 0.001$ and are obtained from the similarity solution without vortex shedding. At this moment, there is just one vortex dipole of the same size of element as that on the wedge surface at its apex. The simulation is then carried out based on the procedure discussed in the previous section. The shed vortex wake is updated through Eq.(8). Figure 2 gives the obtained results. It can be seen that unlike the solution without the vortex wake, the pressure is continuous at the tip. Fig.2 also shows that the variations of the free surface profile and pressure distribution with s in the stretched system are hardly visible. We note that negative pressure exists near the jet root of the left hand side of the wedge. Air could be sucked into the fluid and air cavities could be formed.

Further simulations are carried out with different ε. Fig.3 gives the pressure distribution at $\varepsilon = 0.3,\ 0.5,\ 0.7$. Comparing with the similarity solution without vortex shedding (Xu, Duan & Wu 2008), the pressure jump at the wedge apex has been removed. This is a result of the imposed Kutta condition and vortex wake, through which the flow velocity becomes continuous. The pressure on the left hand side of the wedge is lower than the similarity solution, while the pressure on the right hand side has a lower peak and a smaller slope. We note that when $\varepsilon = 0.7$, the pressure on the left hand side of the wedge has two troughs, which may be due to the flow induced by the shed vortices. Further analysis and results will be provided at the Workshop.

Acknowledgement

The work is mainly supported by Lloyd's Register Foundation (LRF) through the joint centre involving University College London, Shanghai Jiaotong University and Harbin Engineering University, to which the authors are most grateful. LRF helps to protect life and property by supporting engineering-related education, public engagement and the application of research. The first author appreciates the support of NSFC (51479044), China Post-doctor research Fund (2014M560250) and Heilongjiang Post-doctor Research Fund (LBH-Z14057).

References

Battistin D., Iafrati A. 2003 Hydrodynamic loads during water entry of two-dimensional and axisymmetric bodies, Journal of Fluids and Structures 17, 643-664.

Dobrovol'skaya Z.N. 1969 Some problems of similarity flow of fluid with a free surface. Journal of Fluid Mechanics 36, 805-829.

Donwin M.J., Bearman P.W., Graham J.M.R. 1988 Effect of vortex shedding on the coupled roll response of bodies in waves. Journal of Fluid Mechanics 189, 243-264.

Howison S.D., Ockendon J.R., Wilson S.K. 1991 Incompressible water entry problems at small deadrise angles. Journal of Fluid Mechanics 222, 215-230.

Lu C.H., He Y.S., Wu G.X. 2000 Coupled analysis of nonlinear interaction between fluid and structure during impact. Journal of Fluids and Structures 14, 127-146.

Kristiansen T., Faltinsen O.M. 2010 A two-dimensional numerical and experimental study of resonant coupled ship and piston-mode motion. Applied Ocean Research 32, 158-176.

Riccardi G., Iafrati A., 2004 Water impact of an asymmetric floating wedge Journal of Engineering Mathematics 49, 19-39.

Mei X., Liu Y. & Yue D.K.P. 1999 On the water impact of general two-dimensional sections. Applied Ocean Research 21, 1-15.

Korobkin A.A., Iafrati A. 2005 Hydrodynamic loads during initial stage of floating body impact. Journal of Fluids and Structure 21, 413-427.

Semenov Y.A., Iafrati A. 2006 On the nonlinear water entry problem of asymmetric wedges. Journal of Fluid Mechanics 547, 231-256.

Wu G.X., Sun H., He Y.S. 2004 Numerical simulation and experimental study of water entry of a wedge in free fall motion. Journal of Fluids and Structures 19: 277-289.

Xu G.D., Wu G.X. 2013 Boundary element simulation of inviscid flow around an oscillatory foil with vortex sheet, Engineering Analysis with Boundary Elements 37, 825–835.

Xu G.D., Duan W.Y., Wu G.X. 2008 Numerical simulation of oblique water entry of an asymmetrical wedge. Ocean Engineering 35 1597-1603.

Xu G.D., Duan W.Y., Wu G.X. 2010 Simulation of water entry of a wedge through free fall in three degrees of freedom. Proceeding of Royal Society A, 466, 2219-2239.

Zhao R., Faltinsen O.M. 1993 Water entry of two-dimensional bodies. Journal of Fluid Mechanics 246, 593-612.